

A simple algorithm to find the L-curve corner in the regularization of inverse problems

Alessandro Cultrera and Luca Callegaro

ARTICLE HISTORY

Compiled December 9, 2024

ABSTRACT

We propose a simple algorithm devoted to locate the “corner” of an L-curve, a function often used to choose the correct regularization parameter for the solution of many ill-posed problems. The algorithm involves the Menger curvature of a circum-circle and the golden section search method. It efficiently locates the regularization parameter value corresponding to the maximum positive curvature region of the L-curve. The algorithm is applied to some commonly available small test problems and compared to the typical way of locating the L-curve corner by means of its analytical curvature. As a more practical example, the application of the algorithm to the data processing of an electrical resistance tomography experiment on thin conductive films is reported.

KEYWORDS

Image reconstruction, minimization, regularization, reconstruction algorithms, electrical resistance measurement, finite element analysis, tomography.

1. Introduction

The solution $\hat{\mathbf{x}}$ of an ill-posed inverse problem is often formulated in terms of residuals

$$\hat{\mathbf{x}} = \arg \min_{\mathbf{x}} \{ \|\mathbf{A}\mathbf{x} - \mathbf{b}\|^2 \}, \quad \mathbf{A} \in \mathbb{R}^{m \times n}, \quad m > n \quad (1)$$

where the quantity $\mathbf{A}\mathbf{x} - \mathbf{b}$ is the vector of residuals between the experimental data vector \mathbf{b} and the reconstructed data $\mathbf{A}\mathbf{x}$ for a given \mathbf{x} . Regularization techniques are applied to make the problem less sensitive to the noise of \mathbf{b} and find a stable solution. One popular regularization method is to replace the system (1) with

$$\hat{\mathbf{x}}_{\lambda} = \arg \min_{\mathbf{x}} \{ \|\mathbf{A}\mathbf{x} - \mathbf{b}\|^2 + \lambda \mathbf{R}(\mathbf{x}) \}, \quad \lambda \in \mathbb{R}, \quad \lambda \geq 0 \quad (2)$$

where the regularization term $\mathbf{R}(\mathbf{x})$ represents the penalty term in the total cost function, which may include some prior information about the solution. The scalar factor λ is the *regularization parameter*, serving as weighing factor of $\mathbf{R}(\mathbf{x})$. The choice of λ is crucial for the solution to be meaningful. As an example, we consider the regularization method named after Tikhonov [14], in which $\mathbf{R}(\mathbf{x}) = \|\mathbf{x}\|^2$.

A. Cultrera and L. Callegaro are with the Istituto Nazionale di Ricerca Metrologica (INRIM), Strada delle Cacce 91, 10135 Torino, Italy. e-mail: a.cultrera@inrim.it

Several methods (see [6, §. 7]) have been developed in order to find an optimal tuning of λ for a given problem. Of particular interest is the L-curve method (see [6, §. 7.5] and [4]). The L-curve is a two-dimensional curve, parametric in λ , defined by points with cartesian coordinates

$$P(\lambda) = (\xi(\lambda), \eta(\lambda)) \rightarrow \begin{cases} \xi(\lambda) = \log \|\mathbf{Ax} - \mathbf{b}\|^2 \\ \eta(\lambda) = \log \|\mathbf{x}\|^2 \end{cases} \quad (3)$$

The point of maximum positive curvature $P(\lambda_{\text{opt}})$, the “corner”, can be associated to the optimal reconstruction parameter, say λ_{opt} . The underlying concept is that the “corner” represents a compromise between the fitting to the data and the regularization of the solution [7]. Numerical search algorithms have been proposed for the identification of various estimates of λ_{opt} ; among them we mention the splines method [4,8], the triangle method [2] and the L-ribbon method [1]. Here we propose an alternative method which is based on an estimation of the local curvature of the L-curve from three sampled points (which define a circle), and a sampling update rule based on the golden section search. The method attempts to reduce the computational effort by minimizing the number of sampled points of the L-curve explicitly computed. The algorithm is described in detail; an application to a reconstruction problem in electrical resistance tomography is reported.

2. Algorithm

The proposed algorithm 1 is written in pseudo-code. Algorithm 1 calls two functions. The function $P = \text{l_curve.P}(\lambda)$ is based on the the specific regularization problem being solved; it is assumed that at each call, given as input the regularization parameter λ it solves the system (2) and provides as output the point $P(\lambda)$, that is the coordinates $\xi(\lambda)$ and $\eta(\lambda)$ of the L-curve. The function $C_k = \text{menger}(P_j, P_k, P_\ell)$ is defined below in Section 2.1. The algorithm is iterative and identifies our estimate of λ_{opt} , in the following λ_{MC} , by means of the definition of curvature given in Section 2.1 and the golden section search method, described in Section 2.2. “MC” stays for “Menger Curvature”.

2.1. Curvature

The function $C_k = \text{menger}(P_j, P_k, P_\ell)$ is based on the definition of the curvature of a circle by three points given by Menger [11,12]. In our case three values $\lambda_j < \lambda_k < \lambda_\ell$ of the regularization parameter identify three points $P(\lambda_j)$, $P(\lambda_k)$ and $P(\lambda_\ell)$ on the L-curve. Here we follow the notation of (3) for the coordinates of a generic point $P(\lambda)$. For sake of simplicity of notation the substitution (4) is made:

$$\begin{aligned} \xi(\lambda_i) &\rightarrow \xi_i, \\ \eta(\lambda_i) &\rightarrow \eta_i, \\ P(\lambda_i) &\rightarrow P_i. \end{aligned} \quad (4)$$

So we define a signed curvature C_k of the circumcircle as

$$C_k = \frac{2 \cdot (\xi_j \eta_k + \xi_k \eta_\ell + \xi_\ell \eta_j - \xi_j \eta_\ell - \xi_k \eta_j - \xi_\ell \eta_k)}{\left(\overline{P_j P_k} \cdot \overline{P_k P_\ell} \cdot \overline{P_\ell P_j}\right)^{1/2}}, \quad (5)$$

where

$$\begin{aligned} \overline{P_j P_k} &= (\xi_k - \xi_j)^2 + (\eta_k - \eta_j)^2, \\ \overline{P_k P_\ell} &= (\xi_\ell - \xi_k)^2 + (\eta_\ell - \eta_k)^2, \\ \overline{P_\ell P_j} &= (\xi_j - \xi_\ell)^2 + (\eta_j - \eta_\ell)^2, \end{aligned} \quad (6)$$

are the euclidean distances between the sampled L-curve points. Note that we choose to index the curvature with the intermediate index (k) of the three points.

2.2. Golden Section Search

The algorithm is initialized by assigning the search interval $[\lambda_1, \lambda_4]$. Two other values λ_2 and λ_3 are calculated following the golden section method but the calculation is done on the exponents of λ (given $\lambda_i = 10^{x_i}$) in order to maintain a uniform spacing along the many orders of magnitude covered,

$$\begin{aligned} x_2 &= (x_4 + \varphi \cdot x_1)/(1 + \varphi), \\ x_3 &= x_1 + (x_4 - x_2), \end{aligned} \quad (7)$$

where $\varphi = (1 + \sqrt{5})/2$ is the golden section[10]. Four values of λ define four points on the L-curve and allow to calculate two curvatures, C_2 from $\{P(\lambda_1), P(\lambda_2), P(\lambda_3)\}$ and C_3 from $\{P(\lambda_2), P(\lambda_3), P(\lambda_4)\}$. The curvatures C_2 and C_3 are compared; consistent reassignment and recalculation are done in order to work at each iteration with four points $P(\lambda_1) \dots P(\lambda_4)$. The algorithm terminates when the search interval $[\lambda_1, \lambda_4]$ is smaller than a specified threshold ϵ and returns λ_{MC} . This simple exit conditions, the basic choice for the golden section search algorithm, guarantees convergence. More efficient conditions based on the actual $P(\lambda_i)$ coordinates can be implemented.

Note that it may happen that the curvature C_3 associated to the right-hand circle is negative at the initial stage of the search, since C_k is defined with sign in (5). Moreover by definition the corner must always correspond to a positive curvature and it lays on the left-side of the plot. For these reasons the algorithm performs a check, and while $C_3 < 0$ the search extreme λ_1 is kept fixed, λ_4 is shifted toward smaller values and λ_2 and λ_3 are recalculated. The condition on C_3 is strong enough that even in case of both negative curvatures it guarantees the convergence toward the corner.

Some considerations can be done: (a) according to the golden section search method, the algorithm needs to recalculate only one $P(\lambda)$ at each iteration (except for the first iteration), the other can be simply reassigned; this limits the calculation effort; (b) as $P(\lambda_1)$ and $P(\lambda_4)$ are distant at the first iterations, C_2 and C_3 are just rough approximations of the curvature of the L-curve in different regions, but become more accurate as the distance between the search extremes decreases.

Algorithm 1 L-curve corner search

```
1: Initialize  $\lambda_1$  and  $\lambda_4$ ; // search extremes
2: Assign  $\epsilon$ ; // termination threshold
3:  $\varphi \leftarrow (1 + \sqrt{5})/2$ ; // golden section
4:  $\lambda_2 \leftarrow 10^{(x_4 + \varphi \cdot x_1)/(1 + \varphi)}$ ;
5:  $\lambda_3 \leftarrow 10^{x_1 + (x_4 - x_2)}$ ;
6: for  $i = 1$  to 4 do
7:    $P_i \leftarrow \text{l\_curve\_P}(\lambda_i)$ ; // func. l_curve_P returns (3)
8: end for
9: repeat
10:   $C_2 \leftarrow \text{menger}(P_1, P_2, P_3)$ ; // func. menger calls (5)
11:   $C_3 \leftarrow \text{menger}(P_2, P_3, P_4)$ ;
12:  while  $C_3 < 0$  do
13:     $\lambda_4 \leftarrow \lambda_3$ ;  $P_4 \leftarrow P_3$ ;
14:     $\lambda_3 \leftarrow \lambda_2$ ;  $P_3 \leftarrow P_2$ ;
15:     $\lambda_2 \leftarrow 10^{(x_4 + \varphi \cdot x_1)/(1 + \varphi)}$ ;
16:     $P_2 \leftarrow \text{l\_curve\_P}(\lambda_2)$ ;
17:     $C_3 \leftarrow \text{menger}(P_2, P_3, P_4)$ ;
18:  end while
19:  if  $C_2 > C_3$  then
20:     $\lambda \leftarrow \lambda_2$ ; // store  $\lambda$ 
21:     $\lambda_4 \leftarrow \lambda_3$ ;  $P_4 \leftarrow P_3$ ;
22:     $\lambda_3 \leftarrow \lambda_2$ ;  $P_3 \leftarrow P_2$ ;
23:     $\lambda_2 \leftarrow 10^{(x_4 + \varphi \cdot x_1)/(1 + \varphi)}$ ;
24:     $P_2 \leftarrow \text{l\_curve\_P}(\lambda_2)$ ; // only  $P_2$  is recalculated
25:  else
26:     $\lambda \leftarrow \lambda_3$ 
27:     $\lambda_1 \leftarrow \lambda_2$ ;  $P_1 \leftarrow P_2$ ;
28:     $\lambda_2 \leftarrow \lambda_3$ ;  $P_2 \leftarrow P_3$ ;
29:     $\lambda_3 \leftarrow 10^{x_1 + (x_4 - x_2)}$ ;
30:     $P_3 \leftarrow \text{l\_curve\_P}(\lambda_3)$ ; // only  $P_3$  is recalculated
31:  end if
32: until  $(\lambda_4 - \lambda_1)/\lambda_4 < \epsilon$ 
33: return  $\lambda_{\text{MC}} \leftarrow \lambda$ 
```

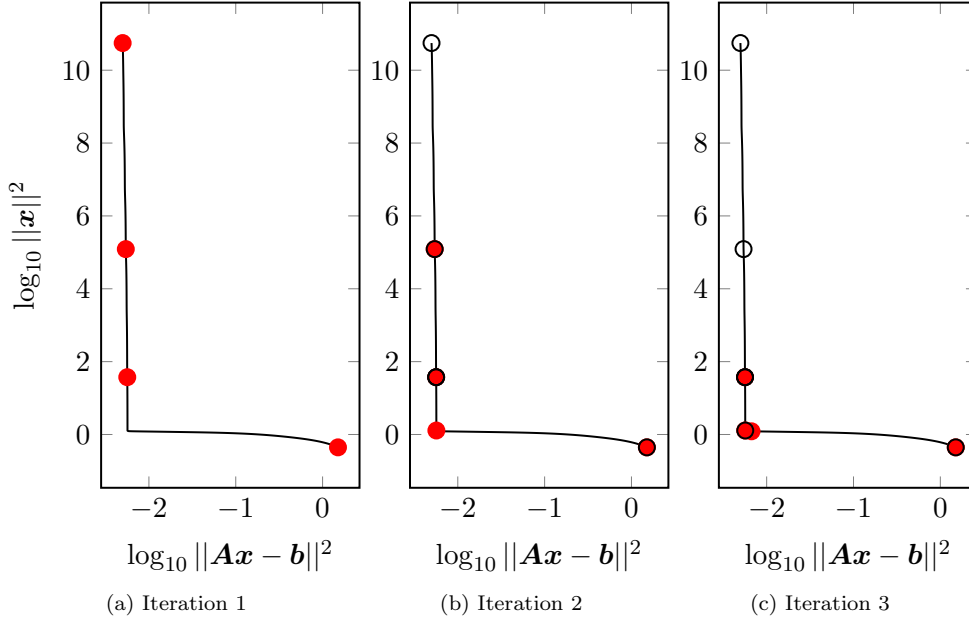


Figure 1. The proposed algorithm at the first three iterations. The reference L-curve is reported as a solid line. Solid circles represent the points $P(\lambda)$ being evaluated at the labeled iteration. Empty circles represent the points evaluated at past iterations. In 1c the four points are no more resolved, see Figure 2 for more detail.

3. Application to test problems

In order to test the algorithm on small demonstrative problems, some (`baart`, `blur`, `shaw` and `spike`) have been chosen from the function library called `Regularization Tools` which is implemented in `MATLAB` [5]. This library is also employed to implement a function used in our algorithm (`L_curve_P(\lambda)`) which evaluates a single point of the L-curve for a given λ . Algorithm 1 is implemented in `MATLAB` as well.

The application of algorithm 1 to the problem `baart` is shown explicitly in the following. This problem represents the discretization of a Fredholm integral equation of the first kind of order n . This means that the matrix \mathbf{A} in (1) is $n \times n$. The chosen size of the problem is $n = 32$. A random noise with a relative standard deviation of 10^{-3} is added to the exact data. The corner of the L-curve generated by this problem is located with both algorithm 1 and the `L_corner` routine from `Regularization Tools`. Figs. 1 and 2 show the evolution of the search for λ_{MC} performed by the algorithm. These figures display also a full L-curve obtained by dense sampling of `L_curve_P(\lambda)` as a reference. The algorithm is run by choosing as initial search extremes same as the standard choice of the `L_corner` routine ($\lambda_1 = 10^{-14}$ and $\lambda_4 = 10^{-1}$). Figure 1 reports three snapshots of the running algorithm. Empty circles represent points visited at previous iterations, while filled circles represent the four points $P_1 \dots P_4$ of the given iteration. Figure 2 shows the detail of the 10th and the 18th (last) iterations. The reader can notice in Figure 2a the L-curve the “corner”. Figure 2b shows the $P(\lambda_i)$ points of the last iteration. Running the algorithm on the other three mentioned problems gives similar results in term of accuracy compared to the native `L_corner` routine of the `Regularization Tools` library. The optimal regularization parameter obtained with this routine is called λ_{RT} in the following. Table 1 summarizes the results of the four test problems with algorithm 1 and the `Regularization Tools`’ function `L_corner`

Table 1. Comparison between algorithm 1 and the analytic curvature approach on test problems.

Problem	λ_{MC}	λ_{RT}	t_{MC} (ms)	t_{RT} (ms)	algorithm 1 iterations
baart(32)	3.92×10^{-3}	4.02×10^{-3}	73	469	18
blur(16,4,5)	3.18×10^{-4}	3.20×10^{-4}	82	459	15
shaw(32)	8.65×10^{-4}	8.28×10^{-4}	69	473	17
spike(32,5)	1.65×10^{-4}	1.60×10^{-4}	61	461	17

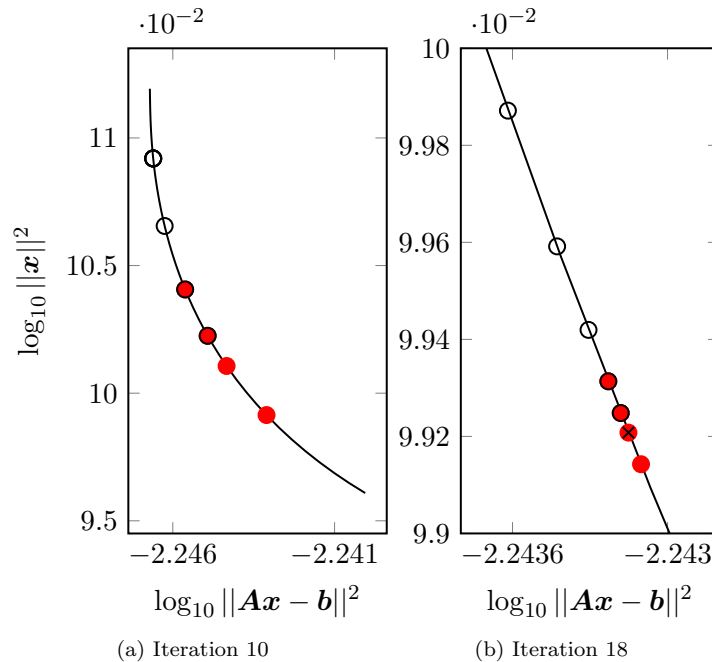


Figure 2. Detail of the corner of the L-curve generated with the `baart` problem. In 2a it is visible the magnified “corner”. In 2b are reported the four $P(\lambda)$ at the last iteration (exit condition $\epsilon = 1\%$). The black \times inside the solid circle marks λ_{MC} .

for each test problem. λ_{MC} is the optimal regularization parameter returned by our algorithm while λ_{RT} is the one returned by the `Regularization Tools` routine. The `MATLAB` profiler was used to get the corresponding net timing¹ of algorithm 1 (t_{MC}), and the `L_corner` routine (t_{RT}). The computational time saving of the proposed algorithm can be ascribed to the fact that the `Regularization Tools` algorithm is based on the solution of an additional optimization problem, the maximization of the analytic curvature [7, §. 5]. Figure 3 shows the evolution of the algorithm towards convergence. Note that, in practical applications, prior knowledge about the problem may allow a restriction of the λ search interval, and the number of iterations can be reduced.

4. Application to Electrical Resistance Tomography

In the following example we apply the algorithm 1 to electrical resistance tomography (ERT), a technique that allows the reconstruction of the conductivity spatial distribu-

¹Eventual plotting time not considered.

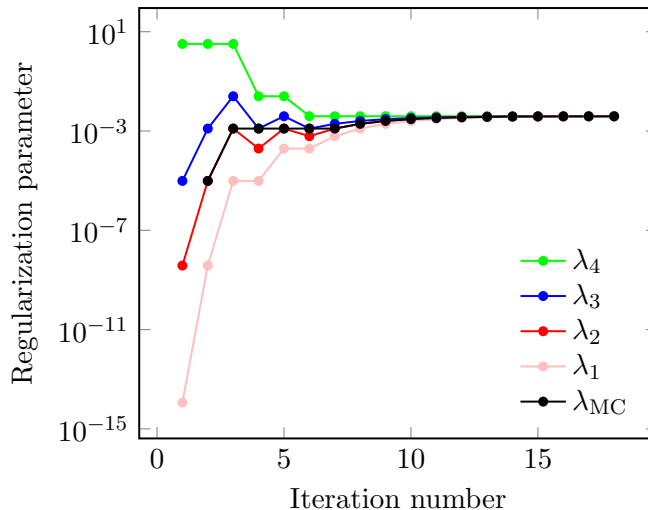


Figure 3. Behaviour of the algorithm versus iteration number for the `baart` problem with a threshold $\epsilon = 1\%$. Black circles (λ_{MC}) represent the λ corresponding to the larger curvature at each iteration.

tion of an object by performing electrical measurements on its boundary. A detailed mathematical formulation of ERT as an inverse problem is given in [9,13].

The specific application, described in detail in [3], concerns the reconstruction of the conductivity map of a thin conductive film sample: a schematic representation of the sample is shown in Figure 6a. The sample has a circular geometry and electrical contacts on the boundary; two circular regions of the film have been ablated, and have therefore zero conductivity. A series of voltage measurements is performed on the contacts, following a protocol described in [3].

Searching a solution following (2), the elements of data vector \mathbf{b} are the voltage values measured at the contacts. The elements of the solution vector \mathbf{x} are the reconstructed discretized conductivity values of the sample. The matrix \mathbf{A} is called *sensitivity matrix* in ERT applications and is constructed from the discretization of the Laplace equation on the sample geometry.

We used EIDORS² routines to generate a two-dimensional circular finite element mesh (2304 elements) with 16 contact points on the mesh boundary (corresponding to a \mathbf{b} of size 208) and compute the matrix \mathbf{A} .

Tikhonov regularization, available in EIDORS, is applied in order to deal with the ill-posed nature of the problem. This formulation is compatible with the calculation of a continuous L-curve and the algorithm described in Section 2.

In Figure 4 are reported the main results of the application of algorithm 1 to ERT experimental data. In Figure 4a are reported the L-curve and the last iteration of algorithm 1. In Figure 4b is reported the detail of the corner. Figure 5 shows the behaviour of the algorithm toward convergence.

The optimal regularization parameter returned by the present algorithm with $\epsilon = 0.01$ is $\lambda_{MC} = 1.764 \cdot 10^{-6}$. This result is used to perform the final image reconstruction shown in Figure 6b. The relative difference between λ_{MC} and λ_{RT} with $\epsilon = 0.01$ is negligible (1 part in 10^{13}). By relaxing the exit condition to $\epsilon = 0.05$, λ_{MC} differs from λ_{RT} by a relative amount of 3 part in 10^3 . This relaxed condition saves 4 iterations (14 instead of 18). In both cases the graphical output would not differ from the image

²Electrical Impedance and Diffuse Optical tomography Reconstruction Software [15].

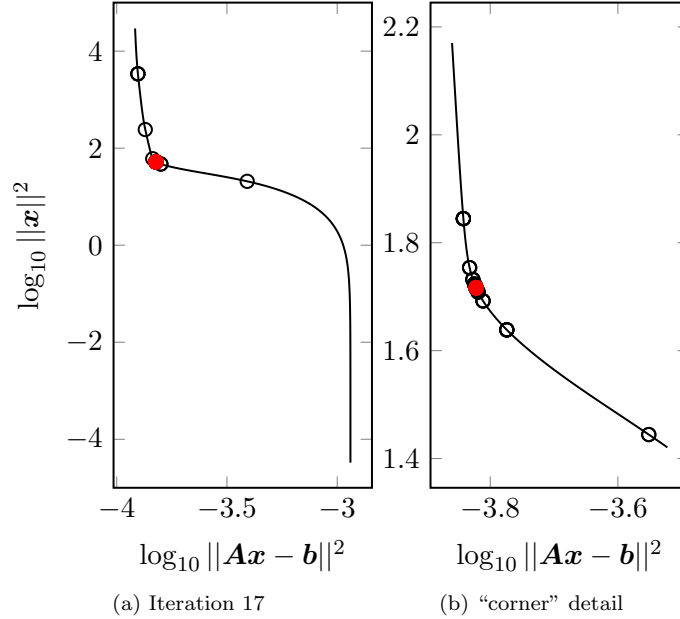


Figure 4. In 4a is reported the L-curve obtained from experimental data and the points corresponding to the last iteration of the algorithm. In 4b is shown the detail of the corner for the experimental data.

reconstruction obtained with λ_{RT} (not shown). Other EIDORS routines are used to graphically render the solution \mathbf{x} as in Figure 6b.

5. Conclusions

The proposed algorithm allows, for a given inverse problem having the form (2), the determination of the regularization parameter λ_{MC} corresponding to the maximum positive curvature of the L-curve. The algorithm is designed for maximum simplicity of implementation on already existing solvers. In both test problems and in a real electrical resistance tomography problem, convergence is achieved in less than 20 iterations, each iteration corresponding to a redetermination of (2). Compared to a common routine for the location of the L-curve corner such as `Regularization Tools` the present algorithm returns strongly compatible results and showed a reduced calculation effort.

6. Acknowledgments

The work is framed within the Joint Research Project 16NRM01 “GRACE: Developing electrical characterisation methods for future graphene electronics”. This project has received funding from the EMPIR programme co-financed by the Participating States and from the European Union’s Horizon 2020 research and innovation programme.

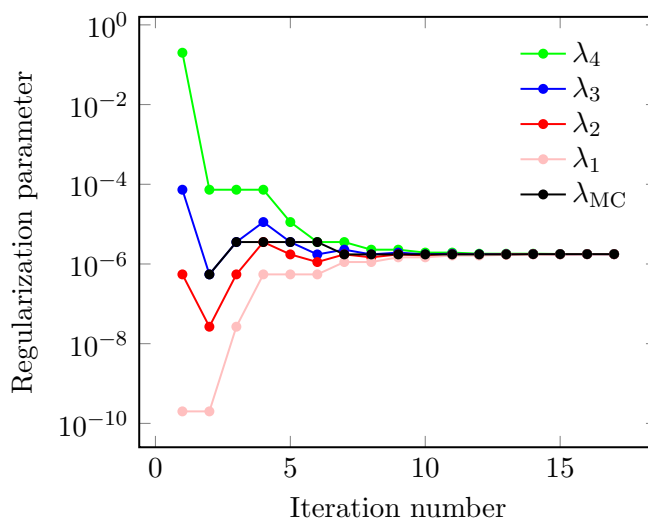
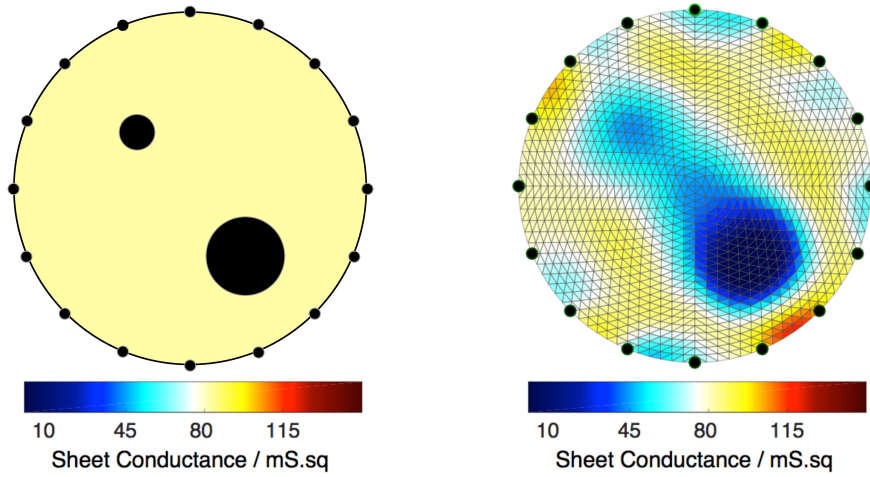


Figure 5. Convergence plot of the algorithm versus iteration number, with a threshold $\epsilon = 1\%$ applied to the ERT experimental data. The last point corresponds to λ_{MC} used in the present image reconstruction.

References

- [1] Calvetti, D., Golub, G. H., and Reichel, L. (1999). Estimation of the L-curve via lanczos bidiagonalization. *BIT Numer. Math.*, **39**(4), 603–619.
- [2] Castellanos, J. L., Gómez, S., and Guerra, V. (2002). The triangle method for finding the corner of the L-curve. *Appl. Numer. Math.*, **43**(4), 359–373.
- [3] Cultrera, A. and Callegaro, L. (2016). Electrical Resistance Tomography of conductive thin films. *IEEE Trans. Instrum. Meas.*, **65**(9), 2101–2107.
- [4] Hansen, P. C. (1992). Analysis of discrete ill-posed problems by means of the L-curve. *SIAM Rev.*, **34**(4), 561–580.
- [5] Hansen, P. C. (1994). Regularization tools: a MATLAB package for analysis and solution of discrete ill-posed problems. *Numer. Algorithms*, **6**(1), 1–35.
- [6] Hansen, P. C. (1998). *Rank-deficient and discrete ill-posed problems: numerical aspects of linear inversion*, volume 4. Siam.
- [7] Hansen, P. C. and O’Leary, D. P. (1993). The use of the L-curve in the regularization of discrete ill-posed problems. *SIAM J. Sci. Comput.*, **14**(6), 1487–1503.
- [8] Hansen, P. C., Jensen, T. K., and Rodriguez, G. (2007). An adaptive pruning algorithm for the discrete L-curve criterion. *J. Comput. Appl. Math.*, **198**(2), 483–492.
- [9] Holder, D. S. (2005). *Electrical Impedance Tomography: Methods, History and Applications*. Series in Medical Physics and Biomedical Engineering. Institute of Physics Publishing, Ltd, London, UK.
- [10] Kiefer, J. (1953). Sequential minimax search for a maximum. *P. Am. Math. Soc.*, **4**(3), 502–506.
- [11] Menger, K. (1930). Untersuchungen über Allgemeine Metrik. *Math. Ann.*, **103**(1), 466–501.
- [12] Pajot, H. (2002). *Analytic capacity, rectifiability, Menger curvature and Cauchy integral*, volume 1799. Springer Science & Business Media.
- [13] Seo, J. K. and Woo, E. J. (2013). *Nonlinear Inverse Problems in Imaging*, chapter Electrical Impedance Tomography, pages 195–249. John Wiley & Sons, Ltd, Chichester, UK.
- [14] Tikhonov, A. N., Goncharsky, A., Stepanov, V., and Yagola, A. G. (2013). *Numerical methods for the solution of ill-posed problems*. Springer Science & Business Media, New York, US.
- [15] Vauhkonen, M., Lionheart, W. R., Heikkinen, L. M., Vauhkonen, P. J., and Kaipio, J. P.

(2001). A MATLAB package for the EIDORS project to reconstruct two-dimensional EIT images. *Physiol. Meas.*, **22**(1), 107.



(a) Scheme of the sample. Colours represent nominal values of sheet conductance.

(b) Sheet conductance map reconstructed from the data with $\lambda_{MC} = 1.764 \cdot 10^{-6}$.

Figure 6. Sheet conductance map obtained with the optimal regularization parameter λ_{MC} returned by our algorithm.